ACS APPLIED MATERIALS & INTERFACES

Research Article

www.acsami.org

Selective Sidewall Wetting of Polymer Blocks in Hydrogen Silsesquioxane Directed Self-Assembly of PS-*b*-PDMS

Richard G. Hobbs, Richard A. Farrell, Ciara T. Bolger, Roisin A. Kelly, Michael A. Morris, Nikolay Petkov,* and Justin D. Holmes*

Materials Chemistry and Analysis Group, Department of Chemistry and the Tyndall National Institute, University College Cork, Cork, Ireland

Centre for Research on Adaptive Nanostructures and Nanodevices (CRANN), Trinity College Dublin, Dublin 2, Ireland

Supporting Information

ABSTRACT: We show the importance of sidewall chemistry for the graphoepitaxial alignment of PS-*b*-PDMS using prepatterns fabricated by electron beam lithography of hydrogen silsesquioxane (HSQ) and by deep ultraviolet (DUV) lithography on SiO_2 thin films. Density multiplication of polystyrene-*block*-polydimethylsiloxane (PS-*b*-PDMS) within both prepatterns was achieved by using a room temperature dynamic solvent annealing environment. Selective tuning of PS and PDMS wetting on the HSQ template sidewalls was also achieved through careful functionalization of the template and substrate surface using either brush or a self-assembled trimethylsilyl monolayer. PDMS selectively wets HSQ sidewalls treated with a brush layer of PDMS, whereas PS is found to selectively wet HSQ sidewalls treated with hexamethyldisilazane (HMDS) to produce a trimethylsilyl-terminated surface. The etch resistance of the aligned polymer was also evaluated to understand the implications of using block copolymer patterns which have high etch resistance, self-forming (PDMS) wetting layers at both interfaces. The results outlined in this work may have direct applications in nanolithography for continued device scaling toward the end-of-roadmap era.

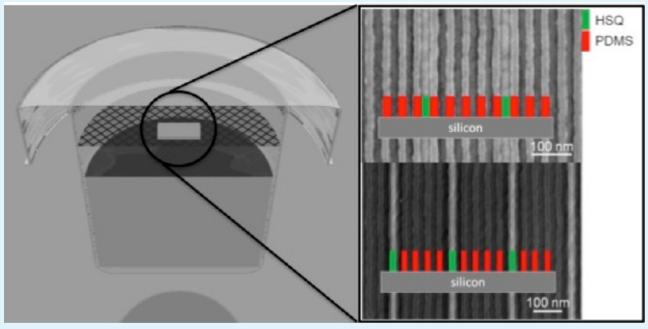

KEYWORDS: *nanolithography, block copolymer, templated self-assembly, surface functionalization, electron beam lithography, hydrogen silsesquioxane*

INTRODUCTION

The drive for continued scaling of semiconductor devices over the last number of decades has put significant pressure on key enabling technologies within the very large scale integrated circuit manufacturing industry, and particularly on the optical lithography techniques used to define semiconductor devices and integrated circuits.[1−3] The use of optical lithography has been extended far beyond the limits of the radiation wavelength through the use of several resolution enhancement techniques.[4] However, as continued scaling becomes significantly more difficult, alternatives to optical lithography are gaining in promise as potential routes to facilitate further scaling.[5−8] Two such alternatives to optical lithography are, electron beam lithography (EBL), and directed self-assembly (DSA) of diblock copolymers. This article describes the use of promising examples of EBL and DSA processes for nanolithography applications, with a view to fabricating high-density arrays of Si nanowires with critical dimensions (CDs) less than 20 nm. The process outlined herein, combines the high density patterning capabilities of block copolymer (BCP) self-assembly with the high-resolution and pattern placement control of EBL. Additionally, the process of DS, within EBL defined templates may negate issues associated with proximity electron scattering effects inherent to high density pattern generation via EBL, by allowing density multiplication within lower density EBL defined templates. This work details the use of hydrogen silsesquioxane (HSQ) as a high-resolution EBL resist for the fabrication of HSQ gratings to act as templates for the DSA of a cylinder-forming PS-*b*-PDMS diblock copolymer.

HSQ is the highest resolution, commercially available, negative-tone EBL resist,[9] and as such is suited to the fabrication of nanoscale structures with sub-10 nm CDs.[10] DSA of BCPs using templates fabricated by traditional lithographic methods is the subject of significant research in the field of advanced lithography.[11,12] PS-*b*-PDMS is a BCP of particular interest in the field of DSA due to its relatively high Flory−Huggins interaction parameter ($\chi \approx 0.26$ at standard temperature and pressure), which can provide sub-10 nm feature sizes and may facilitate reduced line edge roughness (LER) in PS-*b*-PDMS derived structures.[13] Additionally, PDMS

Received: June 5, 2012
Accepted: August 2, 2012
Published: August 2, 2012

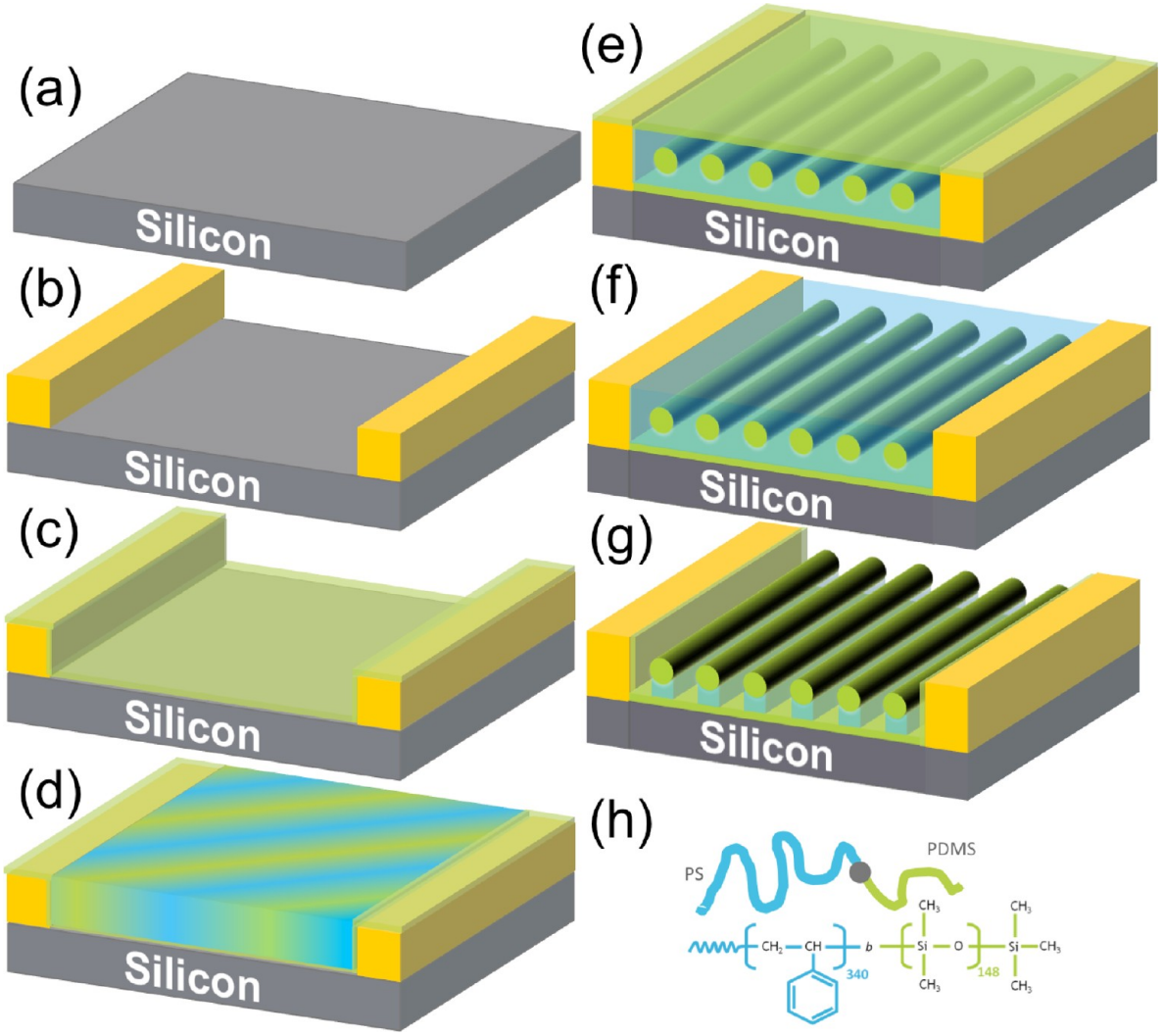

Figure 1. Schematic depiction of the fabrication process used in this work. (a) Si substrate. (b) Template formation via EBL or DUV lithography. (c) Surface functionalization with HMDS or PDMS−OH. (d) Diblock copolymer deposition. (e) Microphase separation of polymer blocks via solvent annealing. (f) PDMS surface etch using CF_4 RIE. (g) PS etch via anisotropic O_2 RIE. (h) Schematic representation of the structure of a PS-b-PDMS diblock copolymer molecule.

offers improved etch resistance relative to analogous organic polymers in conventional reactive ion etch processes.[13] DSA of PS-*b*-PDMS to produce substrate coplanar PDMS gratings has been demonstrated within Si trenches patterned by interference lithography,[13,14] however, this method is not suited to lithography on substrates such as silicon-on-insulator (SOI), where Si trench formation would result in undesirable consumption of the Si device layer. Additionally, using a high resolution EBL technique to pattern the DSA template results in no loss of areal patterning density as both the HSQ line and PDMS cylinder are of comparable feature size. DSA of PS-*b*-PDMS to produce substrate coplanar PDMS gratings using an EBL defined HSQ template has been demonstrated previously using HSQ pillar structures.[15] Similarly, vertical PDMS pillar arrays have been produced via the DSA of PS-*b*-PDMS within an EBL defined HSQ pillar array template.[16] This work identified a strategy to selectively control the wetting of individual blocks in a PS-*b*-PDMS BCP at the template sidewalls for applications of DSA in advanced lithography. Approaches such as that reported by Yamaguchi et al.[17] for selective wetting of polymer blocks of PS-*b*-PMMA within EBL-defined HSQ templates cannot be applied to the PS-*b*-PDMS system as solutions of HSQ in methylisobutyl ketone (MIBK) do not wet PDMS brush-coated substrates unlike the case of PS-*r*-PMMA brush-coated surfaces.

EXPERIMENTAL SECTION

Twenty mm ×20 mm bulk Si ⟨100⟩ oriented substrates, nominal resistivity 0.001 Ω cm, were used for all DSA experiments. The substrates were patterned using a HSQ EBL process prior to deposition of the PS-*b*-PDMS block copolymer (BCP). The substrates were first degreased via ultrasonication in acetone and iso-propanol (IPA) solutions (2 × 2 min), dried in flowing N_2 gas and baked for 2 min at 393 K in an ambient atmosphere to remove any residual IPA. The substrates were then spin coated (500 rpm, 5 s, 2000 rpm, 32 s, lid closed) with a 2.4 wt % solution of HSQ (XR-1541 Dow Corning Corp.) in MIBK to produce a ∼60 nm film of HSQ. The wafer was then baked at 393 K in an ambient atmosphere for 3 min prior to transfer to the EBL system for exposure. Arrays of 15 nm wide lines at pitches of (35n + 15) nm were exposed, where n is an integer and $0 < n < 11$. Following electron beam exposure the samples were developed in an aqueous solution of 0.25 M NaOH, 0.7 M NaCl for 20 s, followed by rinsing in flowing DI water for 60 s. The samples were then blown dry in flowing N_2 gas.

Prior to BCP deposition two approaches were taken to investigate the selectivity between PS and PDMS wetting to the sidewalls of the HSQ template. In both cases the patterned substrate was first cleaned with piranha solution (3/1 v/v 98 wt % H_2SO_4:30 wt % H_2O_2) for 30 min at 358 K, rinsed with DI water, acetone, ethanol and finally blown dry in flowing N_2 gas. Prior to PDMS brush or hexamethyldisilazane (HMDS) deposition, the substrate surface was partially oxidized using an O_2 RIE in an Oxford Plasmalab 100 using the following parameters: 100 W platen power, 1 mTorr chamber pressure, and 40 sccm O_2 flow rate for 20 s. The first approach to investigate wetting selectivity was to apply a 5 kg mol^{-1} brush layer of monocarbinol terminated PDMS (PDMS−OH) to the substrate. The substrate was first covered with the working solvent, CCl_4, and spun dry to improve adhesion of the PDMS−OH solution. PDMS−OH, filtered through a 0.2 μm mesh, was then deposited by spin coating (3000 rpm, 20 s) a solution of 0.5 wt % PDMS−OH. The substrate was then annealed at 423 K for 15 h under vacuum to facilitate chemical grafting of PDMS−OH to the Si−OH surface via a condensation reaction. The substrate was then allowed to cool and the excess PDMS−OH was removed by ultrasonication in toluene at 323 K for 10 min. A second approach to investigate wetting selectivity was to coat the substrate with HMDS by immersing the substrate in HMDS for 2 min. HMDS reacts with hydroxyl terminated Si according to the reaction scheme given in eq 1.[18]

$$2{\equiv}SiOH + (CH_3)_3Si - NH - Si(CH_3)_3 \rightarrow 2{\equiv}SiOSi(CH_3)_3 + NH_3 \quad (1)$$

The reaction scheme given in eq 1 yields a trimethysilyl terminated surface.

Following surface treatment of the patterned substrates the PS-*b*-PDMS BCP (34 kg mol^{-1}-b-11 kg mol^{-1}) was deposited according to the following procedure: PS-*b*-PDMS (0.5 wt % in CCl_4) was spin coated onto the treated substrates (6000 rpm, 20 s) and annealed in toluene vapor for 4−16 h using an apparatus such as that shown in the Supporting Information, Figure S1.

Solvent annealing was performed in a 5 cm inner diameter glass jar containing a toluene reservoir. The substrate was placed on a steel mesh sitting 1 cm above the surface of the toluene reservoir and 2−3 mm below the lip of the jar. The jar was capped with a downturned glass Petri dish so as to allow a slow leak of toluene vapor (~1 cm^3 h^{-1}). The samples were then etched, anisotropically, in two steps following solvent annealing, as shown schematically in Figure 2. The first etch step used a CF_4/O_2 reactive ion etch (RIE) in an STS Advanced Oxide Etcher system to etch the surface PDMS layer. The etch used 100 W platen power, 1 mTorr chamber pressure, CF_4 flow rate of 30 sccm, and O_2 flow rate of 8 sccm for 30 s. The second RIE step to anisotropically etch the PS layer through to the underlying PDMS layer, used the following parameters: platen power 100 W, chamber pressure 1 mTorr, and O_2 flow rate 40 sccm for 20 s.

The SiO_2 trenches used in this study were fabricated using a series of lithography and etch steps. The final oxide depth of the trench was 30 nm and the trench width was 280 nm. Photoresist patterns with large line/space features were exposed with DUV lithography on 30 nm thick SiO_2 films to create trenches with large mesas. The photoresist patterns were transferred to the underlying SiO_2 film via RIE.

Critical dimensions and LER of line structures fabricated in this work were determined from analysis of SEM images using ImageJ software as described previously.[19]

RESULTS

HSQ gratings prepared by EBL, and patterned SiO_2 coated Si substrates were used as templates to direct the self-assembly of PS-*b*-PDMS diblock copolymer films. Figure 1 displays a process flow diagram of the fabrication process used in this work including a schematic representation of the sequential etch processes employed to generate a PDMS grating from a microphase separated film of PS-*b*-PDMS. Figure 1 also illustrates a schematic representation of the molecular structure of the PS-*b*-PDMS diblock copolymer and the orientation of the diblock copolymer film after microphase separation.[14] A thin film of PDMS forms at the BCP−air interface and at the substrate−BCP interface due to the low surface tension of PDMS (19.9 mN m^{-1}) with respect to PS (40.7 mN m^{-1}).[20]

Two surface functionalization approaches were used to prepare aligned BCP films by DSA. In the first approach, a hydroxyl-terminated PDMS−OH brush layer was chemically grafted to the patterned Si or SiO_2 substrate as described above. The PDMS−OH brush layer binds to the hydroxyl-terminated substrate via a condensation reaction.[21] However, as the PDMS−OH brush is deposited globally, i.e., on both the trench floor and the template sidewalls, it was observed that the PDMS component of the BCP preferentially adhered to the template sidewalls, as shown in Figures 3 and 4. PDMS is chemically very similar to HSQ given that they both consist of an inorganic (SiO_x) subsystem. This chemical similarity between HSQ and PDMS makes selective etching of one with respect to the other very difficult, and as such HSQ lines cannot be selectively removed to allow production of a uniform grating after PS etching. Production of uniform nanoscale gratings is desirable for applications such as nanowire array fabrication. However, as there is no known etch procedure that can selectively etch HSQ with respect to PDMS, or vice versa the process outlined above would result in the formation of a grating mask with variable line-width following PS etching. Consequently, another approach had to be considered to prevent PDMS adhesion to the template sidewalls like that seen in Figures 3 and 4. One possible approach to prevent preferential wetting of PDMS at the HSQ template sidewalls, would be to use a PS brush layer in lieu of a PDMS brush layer, which may allow selective wetting of PS at the template sidewall.[14] However, difficulties have been associated with the use of a PS brush layer for the PS-*b*-PDMS system, which have been attributed to poor diffusivity of PDMS on PS-coated surfaces.[14] As an alternative to the use of a PDMS or PS brush, hexamethyldisilazane (HMDS) was applied to a patterned substrate as described above. The additional surface methyl groups produced at a HMDS treated surface, relative to a PDMS treated surface, were expected to improve wetting of the organic PS component of the BCP. Furthermore, the use of HMDS instead of PS or PDMS brush layers should reduce demands on etching processes used to transfer BCP microphase patterns to the substrate as HMDS produces a monolayer of trimethylsilyl species, which is significantly thinner than PS or PDMS brush layers. Figure 2 shows SEM images of a PDMS 'fingerprint' pattern typically produced in the absence of a template to direct microphase separation. The SEM images displayed in Figure 2 were recorded following sequential CF_4 and O_2 RIE steps to etch the upper PDMS layer and underlying PS layers respectively. The "fingerprint" patterns observed in Figure 2 illustrate that both PDMS and HMDS treated surfaces result in identical microphase separated PS-*b*-PDMS thin film morphologies.

Figure 3 displays SEM images of aligned PDMS lines within SiO_2 trenches where (a) is HMDS coated and (b) PDMS−OH coated. Successful alignment was observed for both PDMS−OH brush coated and HMDS treated substrates. Figure 3a clearly shows that PS wets the sidewalls of the HMDS-treated SiO_2 trench given the observed gap between the PDMS lines and the trench walls in the displayed SEM image. Aligned PDMS lines are also observed on the mesas of the substrate in

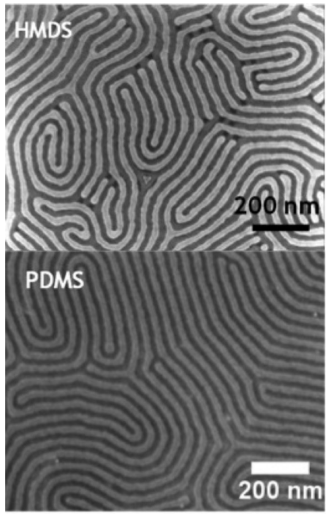

Figure 2. SEM images of PDMS "fingerprint" patterns produced by the self-assembly of PS-*b*-PDMS on a Si substrate treated with either a PDMS brush layer or silylated by immersion in HMDS. The SEM images were captured following the reactive ion etch process outlined in Figure 1 to remove the PDMS overlayer and PS matrix.

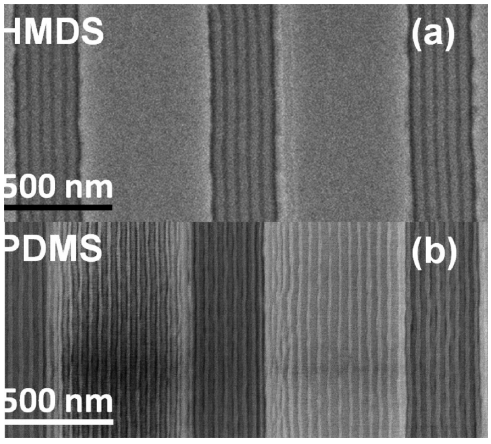

Figure 3. SEM images of aligned PDMS gratings within three PDMS−OH and HMDS coated trenches in a SiO_2 film on a Si substrate.

the case of the PDMS coated sample, which may be related to the higher diffusivity of the BCP on PDMS surfaces. The SEM images in Figure 3 were recorded following sequential RIE steps to etch the surface PDMS layer and underlying PS layers, respectively.

A range of different HSQ line patterns were prepared by EBL for DSA experiments. HSQ line arrays (10 × 10 μm) were exposed with a line-width of 15−20 nm, at pitches of 65, 100, 135, 205, 275, 345, and 415 nm, which required exposure doses of 1.1, 1.4, 1.7, 2.0, 2.4, 2.7, and 3.0 mC cm^{-2}, respectively. The HSQ line pitch was increased in multiples of the expected 35 nm PDMS cylinder periodicity (L_0).[22] Figure 4 shows an SEM image of PS-*b*-PDMS alignment within PDMS brush-coated HSQ gratings, following a CF_4 RIE to remove the top PDMS layer and an O_2 RIE to anisotropically etch PS. The result shows a repeating 60 nm wide PDMS-HSQ-PDMS line structure interspersed within the array of 20 nm wide PDMS lines. The average measured PDMS L_0, width and edge roughness were 38.5 19.6, and 4.3 nm respectively. Figure 4b displays an SEM image of BCP alignment within HMDS-

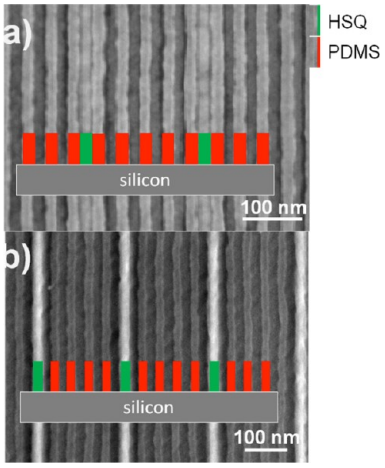

Figure 4. SEM images of aligned PDMS lines within a grating of 22 nm wide HSQ lines at a pitch of 205 nm on (a) a PDMS brush coated surface, and (b) a HMDS treated surface.

coated HSQ gratings, following CF_4 and O_2 RIE processes. The SEM image clearly shows that PDMS no longer preferentially wets the sidewalls of the HSQ lines and as such facilitates the fabrication of a uniform mask grating. The average PDMS L_0, width and edge roughness were measured at 39.4, 19.3, and 5.0 nm respectively for this process.

Figure 5 displays a lower-magnification SEM image of PDMS alignment on a PDMS−OH coated surface, than that in Figure

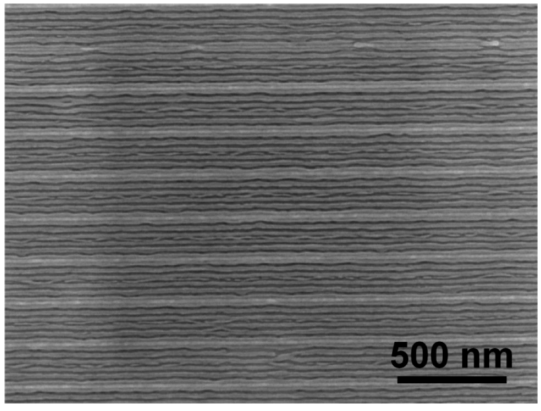

Figure 5. SEM image of a ~5 μm^2 area of aligned PDMS lines, within a template of 15 nm HSQ lines, at a pitch of 190 nm.

4. The SEM image in Figure 5 shows an array of PDMS lines within a template of 15 nm wide HSQ lines at a pitch of 190 nm. The sample has been partially etched in an identical fashion to the films shown in Figure 4, and shows good alignment over the area shown. Lines of material are seen to overlay regions where trenches are expected in the SEM image in Figure 5. The observed material may be attributable to incomplete removal of the surface PDMS layer during the CF_4 RIE process. Despite the incomplete removal of material within the trenches of the BCP film, alignment of PDMS can be seen over the ~5 μm^2 area.

Figure 6 displays a TEM image of a cross-section through the line grating shown in Figure 4b. The TEM image clearly shows the uniform 5 nm thick PDMS layer on the trench base. The TEM image also shows the profile of the HSQ and PDMS line grating. The PS/PDMS lines are 10 nm high and approximately

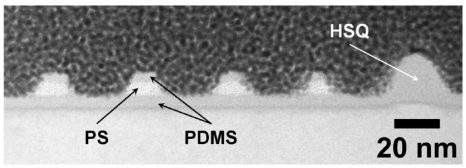

Figure 6. TEM image of a cross-section through aligned PDMS lines within a grating of 22 nm wide HSQ lines at a pitch of 205 nm on a HMDS treated surface.

17 nm wide at the base. The HSQ line is 22 nm high, which is significantly less than the initial thickness of 50 nm expected after EBL. However, HSQ is known to etch at a rate of over 20 nm min^{-1} in a similar CF_4 RIE to that used in this work.[23] Consequently, significant consumption of the HSQ template can be expected during the CF_4 RIE procedure.

A HSQ line pitch of 205 nm was observed to produce the best alignment of BCP for both HMDS and PDMS-treated substrates, due to the observed L_0 of 39 nm for aligned PS-b-PDMS as measured via SEM inspection in figure 4. The PS-*b*-PDMS film produced consists of 19 nm diameter PDMS cylinders separated by 20 nm PS lines, in contrast to the L_0 of 35 nm that had been expected. Taking the actual PS-*b*-PDMS periodicity of 39 nm into account, a HSQ template with trench widths of $nL_0 + b_w$ would now be expected to support DSA, where '*n*' represents a nonzero positive integer, and b_w represents the width of the polymer block which wets the template sidewall. This description of the trench width agrees with the observed DSA within the template having a pitch of 205 nm. A trench width of 176 nm is predicted when $n = 4$, and PS wets the template sidewall. A trench width of 176 nm translates to a HSQ line pitch of approximately 205 nm when the 22 nm HSQ line width and template functionalization layers are additionally considered.

CONCLUSIONS

High resolution EBL using a HSQ EBL resist has been used to guide the microphase separation of PS-*b*-PDMS by a process of DSA. A process has been developed to improve wetting of PS to the HSQ template with respect to PDMS, thus allowing the fabrication of uniform 20 nm lines at a pitch of ~40 nm. The degree of BCP alignment within the HSQ templates was observed to depend significantly on the trench width of the template. The demonstrated importance of template dimensions and surface treatment suggests that there is also a chemical component to graphoepitaxy, which must be considered when designing substrates, especially when creating regular line arrays. The HSQ templates prepared by EBL have also been shown to allow the creation of line arrays with varied critical dimensions by controlling the template sidewall chemistry.

ASSOCIATED CONTENT

Supporting Information

A schematic representation of the apparatus used for the solvent annealing of block copolymer films is included. This material is available free of charge via the Internet at http://pubs.acs.org.

AUTHOR INFORMATION

Corresponding Author

*Tel: +353 (0)21 4903608. Fax: +353 (0)21 4274097. E-mail: j.holmes@ucc.ie (J.D.H.); nikolay.petkov@tyndall.ie (N.P.).

Notes

The authors declare no competing financial interest.

ACKNOWLEDGMENTS

We acknowledge financial support from the Irish Research Council for Science, Engineering and Technology (IRCSET) and Science Foundation Ireland (Grants: 08/CE/I1432, 09/IN.1/602 and 09/SIRG/I1621). This research was also enabled by the Higher Education Authority Program for Research in Third Level Institutions (2007-2011) via the INSPIRE programme. The authors would like to thank Intel Ireland for provision and development of patterned wafers under the Adaptive Grid Substrate CRANN programme. We also acknowledge the National Access Program (NAP) for access to electron beam lithography provided by Tyndall National Institute (NAP 148/248).

REFERENCES

(1) *International Technology Roadmap for Semiconductors: 2010 Update Overview*; http://www.itrs.net/Links/2010ITRS/2010Update/ToPost/2010_Update_Overview.pdf.
(2) Service, R. F. *Science* **2009**, *323*, 1000.
(3) Pease, R. F.; Chou, S. Y. *Proc. IEEE* **2008**, *96*, 248.
(4) French, R. H.; Tran, H. V. *Annu. Rev. Mater. Res.* **2009**, *39*, 93.
(5) Hobbs, R. G.; Petkov, N.; Holmes, J. D. *Chem. Mater.* **2012**, *24*, 1975.
(6) Berggren, K. K.; Bard, A.; Wilbur, J. L.; Gillaspy, J. D.; Helg, A. G.; McClelland, J. J.; Rolston, S. L.; Phillips, W. D.; Prentiss, M.; Whitesides, G. M. *Science* **1995**, *269*, 1255.
(7) Chou, S. Y.; Xia, Q. *Nat. Nanotechnol.* **2008**, *3*, 295.
(8) Cavallini, M.; D'Angelo, P.; Criado, V. V.; Gentili, D.; Shehu, A.; Leonardi, F.; Milita, S.; Liscio, F.; Biscarini, F. *Adv. Mater.* **2011**, *23*, 5091.
(9) Grigorescu, A. E.; Hagen, C. W. *Nanotechnology* **2009**, *20*, 292001.
(10) Manfrinato, V. R.; Cheong, L. L.; Duan, H.; Winston, D.; Smith, H. I.; Berggren, K. K. *Microelectron. Eng.* **2011**, *88*, 3070.
(11) Herr, D. J. C. *J. Mater. Res.* **2011**, *26*, 122.
(12) Darling, S. B. *Prog. Polym. Sci.* **2007**, *32*, 1152.
(13) Jung, Y. S.; Chang, J. B.; Verploegen, E.; Berggren, K. K.; Ross, C. A. *Nano Lett.* **2010**, *10*, 1000.
(14) Jung, Y. S.; Ross, C. A. *Nano Lett.* **2007**, *7*, 2046.
(15) Yang, J. K. W.; Jung, Y. S.; Chang, J.-B.; Mickiewicz, R. A.; Alexander-Katz, A.; Ross, C. A.; Berggren, K. K. *Nat. Nanotechnol.* **2010**, *5*, 256.
(16) Bita, I.; Wang, J. K. W.; Jung, Y. S.; Ross, C. A.; Thomas, E. L.; Berggren, K. K. *Science* **2008**, *321*, 939.
(17) Yamaguchi, T.; Yamaguchi, H. *Adv. Mater.* **2008**, *20*, 1684.
(18) Gun'ko, V. M.; Vedamuthu, M.; Henderson, G.; Blitz, J. *J. Colloid Interface Sci.* **2000**, *228*, 157.
(19) Hobbs, R. G.; Schmidt, M.; Bolger, C. T.; Georgiev, Y. M.; Fleming, P.; Morris, M. a.; Petkov, N.; Xiu, F.; Wang, K. L.; Djara, V.; Yu, R.; Colinge, J.-P.; Holmes, J. D. *J. Vac. Sci. Technol. B* **2012**, *30*, 041602.
(20) Jung, Y. S.; Jung, W.; Ross, C. A. *Nano Lett.* **2008**, *8*, 2975.
(21) Granville, A. M.; Brittain, W. J. In *Polymer Brushes: Synthesis, Characterization, Applications*; Advincula, R. C.; Brittain, W. J.; Caster, K. C.; Ruhe, J., Eds.; Wiley-VCH Verlag Gmbh & Co.: Weinheim, Germany, 2004; pp 35−50.
(22) Jung, Y. S.; Jung, W.; Tuller, H. L.; Ross, C. a *Nano Lett.* **2008**, *8*, 3776.

(23) Yang, J. K. W.; Anant, V.; Berggren, K. K. *J. Vac. Sci. Technol., B* **2006**, *24*, 3157.